Spectrum of Engineering Sciences
ISSN (e) 3007-3138 (p) 3007-312X Volume 4, Issue 3, 2026

THE INFLUENCE OF STEEL AND GLASS FIBER ADDITION ON SHEAR STRENGTH OF BEAM–COLUMN CONNECTIONS IN REINFORCED CONCRETE: AN EXPERIMENTAL INVESTIGATION

[1]Dr. M. Adil Khan, [2]Engr. Waseem Ashraf, [3]Rao Ahmar Arshad, [4]Usama Bin Umer, [5]Muhammad Mudassar Abbas*, [6]Muhammad Saad Imran, [7]Uzair Ali

[1]Resident Engineer (RE), National Engineering Services Pakistan (NESPAK), Lahore, Pakistan
[2]Project Manager, Sheikh Abdur Razaq Construction Company (SARCO), Punjab, Pakistan
[3]National Institute of Transportation (NIT), National University of Science and Technology (NUST), Islamabad, Pakistan
[4]Department of Civil Engineering, University of Engineering and Technology (UET), Taxila, Pakistan
[5]Department of Civil Engineering, University of Engineering and Technology, Taxila, Pakistan
[6]National University of Science and Technology (NUST), Islamabad, Pakistan
[7]Local Government and Rural Development Department, Khyber Pakhtunkhwa, Pakistan
[1]adee.uol@gmail.com, [2]wasi0625@yahoo.com, [3]raoahmar235@gmail.com, [4]usama558084@gmail.com, [5]engrmudassar91@gmail.com, [6]si1717e@gmail.com, [7]engruzair91@gmail.com

Keywords
Beam–column connection, shear strength, steel fibers, glass fibers, reinforced concrete, ductility, seismic performance

Article History
Received on 26 Feb, 2026
Accepted on 13 March, 2026
Published on 15 March, 2026

Corresponding Author
Muhammad Mudassar Abbas

Abstract

Beam–column connections represent the most critical regions in reinforced concrete (RC) moment-resisting frames, particularly under seismic loading conditions. These joints are susceptible to brittle shear failure due to high stress concentrations and reinforcement congestion, which often compromises concrete consolidation. This experimental investigation evaluates the efficacy of discrete steel and glass fibers as supplementary reinforcement to enhance the shear strength and ductility of exterior beam–column connections. Nine full-scale specimens were cast and tested under monotonic loading, comprising one control specimen, four steel fiber-reinforced concrete (SFRC) specimens, and four glass fiber-reinforced concrete (GFRC) specimens. Fiber volume fractions ranged from 0.5% to 2.0%. The results indicate that the inclusion of fibers significantly alters the failure mode from brittle shear to a more ductile flexural mechanism. Steel fibers demonstrated superior performance in ultimate load capacity and energy dissipation, while glass fibers provided effective crack control and stiffness retention at lower costs. The study concludes that fiber reinforcement can partially replace traditional transverse steel in joint cores, offering a viable solution for seismic retrofitting and simplified construction in congested regions.

1. Introduction

The structural integrity of reinforced concrete (RC) frames relies heavily on the performance of beam–column connections. In moment-resisting frames designed according to modern seismic codes, the prevailing design philosophy is "strong column–weak beam," intended to force plastic hinging into the beams rather than the columns or joints. However, despite these design provisions, beam–column joints remain vulnerable to shear failure during severe earthquake events. This vulnerability stems from the complex stress state within the joint core, where forces from the beam and column intersect, generating high diagonal tensile stresses that concrete alone cannot resist (de Sousa et al., 2022).

Traditionally, shear resistance in joint regions is provided by transverse reinforcement (stirrups or ties). While effective, the placement of dense transverse reinforcement in the joint core often leads to severe reinforcement congestion. This congestion complicates the construction process, hinders the proper flow and consolidation of concrete, and may ultimately result in honeycombing or voids that weaken the joint (Vallurupalli et al., 2021). Consequently, there is a growing interest in alternative reinforcement strategies that can mitigate congestion while maintaining or enhancing structural performance.

Discrete fiber reinforcement has emerged as a promising solution to this challenge. By distributing short, discrete fibers throughout the concrete matrix, the post-cracking tensile strength and toughness of the composite material are significantly improved. Fibers act as crack arrestors, bridging micro-cracks before they propagate into macro-cracks, thereby enhancing the shear transfer capacity across crack interfaces (Turlapati & Vineel, 2020). Two of the most common fiber types utilized in structural applications are steel fibers and glass fibers. Steel fibers, typically made of high-strength carbon steel with hooked or deformed ends, provide substantial tensile strength and ductility. Conversely, alkali-resistant (AR) glass fibers offer high tensile strength and corrosion resistance at a lower weight and cost, though they generally exhibit lower modulus of elasticity compared to steel (Ganesan et al., 2025).

While the behavior of fiber-reinforced concrete (FRC) in beams and columns has been extensively documented, its application specifically within beam–column joints require further investigation. The joint region experiences a unique triaxial stress state that differs from standard flexural members. Previous studies, such as those by (Shoukry et al., 2023), have suggested that fiber addition can delay shear cracking and improve energy dissipation. However, a comparative analysis between steel and glass fibers within the same experimental framework remains limited in the literature. Furthermore, the quantification of the contribution of fibers to the nominal shear strength of the joint, relative to traditional transverse reinforcement, is necessary for the development of updated design provisions.

This paper presents a comprehensive experimental investigation into the influence of steel and glass fiber addition on the shear strength of exterior beam–column connections. The primary objectives of this study are:

(1) to evaluate the crack propagation patterns and failure modes of fiber-reinforced joints compared to conventional RC joints;

(2) to quantify the enhancement in ultimate load capacity and stiffness resulting from varying volume fractions of steel and glass fibers;

(3) to assess the ductility and energy absorption capabilities of the specimens; and

(4) to compare the experimental shear strengths with theoretical predictions based on existing code provisions. By addressing these objectives, this research aims to provide empirical data supporting the use of FRC as a viable method for optimizing joint design in seismic regions.

2. Literature Review

The behavior of beam–column joints has been a subject of intense research since the recognition of joint shear failures following major earthquakes in the 1970s. Early work by Paulay and Priestley (1992) established the fundamental mechanics of joint shear transfer, identifying the diagonal compression strut mechanism and the contribution of truss action provided by stirrups.

However, the reliance on steel ties for shear resistance introduces constructability issues (Goksu, 2021). As noted by Hegger et al. (2009), the density of reinforcement in high-seismic zones often exceeds practical placement limits, leading to quality control issues during casting.

The introduction of discrete fibers into concrete matrices was initially focused on industrial flooring and precast elements. Over the last two decades, research has shifted toward structural applications. Zaidir & Wardi (2023) conducted a seminal review on the use of fiber-reinforced concrete in seismic applications, concluding that fibers significantly improve the deformation capacity of structural members. Specifically, in shear-critical regions, fibers provide a residual tensile strength after the concrete matrix cracks, which maintains aggregate interlock and dowel action.

Regarding steel fibers, numerous studies have confirmed their efficacy in joint regions. Asheghi Mehmandari et al. (2024) tested exterior beam–column joints reinforced with hooked-end steel fibers and observed a shift from brittle shear failure to ductile flexural failure. The study reported an increase in joint shear strength of up to 40% with a fiber volume fraction of 1.5%. Similarly, Sarmiento et al. (2019) investigated high-strength SFRC joints and found that steel fibers could effectively replace a portion of the transverse reinforcement without compromising safety margins. The mechanism is attributed to the fiber bridging effect, which resists the opening of diagonal tension cracks that typically precipitate joint failure.

Glass fiber reinforcement, while less common in primary structural members due to concerns regarding alkali-silica reaction and long-term durability, has gained traction with the development of Alkali-Resistant (AR) glass fibers. Zaidir & Wardi (2023) demonstrated that GFRC exhibits excellent tensile strain capacity, making it suitable for controlling crack widths. In the context of beam–column joints, (Lee et al., 2022) conducted a comparative study of steel and glass fibers. Their results indicated that while steel fibers provided higher ultimate loads, glass fibers were effective in enhancing the first crack load and stiffness, offering a cost-effective alternative for moderate seismic zones.

Recent advancements have also focused on hybrid fiber systems. Kesavamoorthi & Ganesh (2024) explored the combination of macro and micro fibers, suggesting that a multi-scale reinforcement approach can optimize both early-age cracking and ultimate load capacity. However, the complexity of hybrid mixes often complicates quality control in field applications. Therefore, understanding the performance of single-fiber type systems remains crucial for practical implementation.

Despite these advancements, gaps remain in the standardization of design equations. Current building codes, such as ACI 318-19, do not explicitly account for the contribution of discrete fibers to the shear strength of beam–column joints in design calculations, often treating them as a safety margin rather than a design component (Li et al., 2022). This conservative approach limits the widespread adoption of FRC in joint design. This study seeks to contribute data that bridges the gap between experimental observation and code-based design, specifically comparing the efficacy of steel versus glass fibers in full-scale joint specimens.

3. Experimental Program

3.1. Specimen Design and Geometry

The experimental program consisted of nine full-scale exterior beam–column sub-assemblages. The geometry of the specimens was designed to represent a typical interior frame joint scaled for laboratory testing capabilities, adhering to standard proportions found in mid-rise residential structures. Each specimen comprised a vertical column segment and a horizontal beam segment cast monolithically.

The column dimensions were 300 mm × 300 mm with a total height of 2000 mm. The beam dimensions were 250 mm × 300 mm with a length of 1500 mm from the face of the column. The joint core dimensions were consequently 300 mm × 300 mm × 250 mm (depth). All specimens were reinforced with longitudinal deformed steel bars of grade 420 MPa yield strength. The beam reinforcement consisted of three 16 mm diameter bars at the top and bottom, while the column contained four 20 mm diameter bars. To isolate the effect of fibers on shear strength, the transverse reinforcement (stirrups) within the joint core was minimized to the code-specified minimum, ensuring that any increase in shear capacity could be attributed to the fiber contribution rather than additional steel ties.

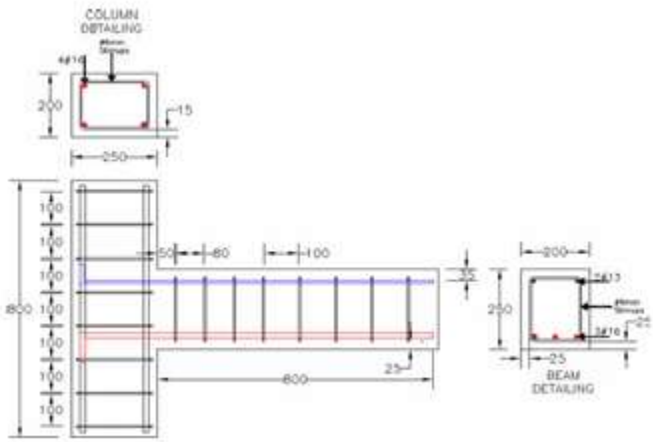

Figure 1: Reinforcement Detailing

A detailed schematic diagram showing the dimensions of the beam-column specimen. The diagram indicates the column height (2000mm), beam length (1500mm), cross-sectional dimensions, and the placement of longitudinal reinforcement. A detailed inset shows the joint core region with minimal stirrup spacing.

3.2. Material Properties

The concrete mix design targeted a compressive strength (f'_c) of 35 MPa at 28 days. Ordinary Portland Cement (Type I) was used with a water-cement ratio of 0.45. The coarse aggregate consisted of crushed limestone with a maximum size of 12 mm to facilitate fiber dispersion and prevent balling. Fine aggregate was natural river sand.

Two types of fibers were utilized:

1. **Steel Fibers:** Hooked-end steel fibers with a length of 30 mm and a diameter of 0.5 mm (aspect ratio $l/d = 60$). The tensile strength of the steel fibers was 1100 MPa.
2. **Glass Fibers:** Alkali-resistant (AR) glass fibers bundled in strands, chopped to a length of 12 mm. The tensile strength was approximately 1700 MPa.

The fibers were added by volume fraction (Vf). For steel fibers, the content was calculated by weight of concrete, while for glass fibers, it was calculated by weight of cement to ensure proper dispersion, following the methodology of Qureshi and Muhammad (2018).

Table 1: *Mix proportions and specimen identification Details*

Specimen ID	Fiber Type	Volume Fraction (Vf)	Concrete Strength (f'c) MPa
CJ-0	None (Control)	0.0%	36.5
SF-05	Steel	0.5%	37.2
SF-10	Steel	1.0%	38.1
SF-15	Steel	1.5%	37.8
SF-20	Steel	2.0%	36.9
GF-05	Glass	0.5%	35.8
GF-10	Glass	1.0%	36.2
GF-15	Glass	1.5%	35.5
GF-20	Glass	2.0%	35.1

3.3. Mixing and Curing

The mixing procedure was critical to ensure uniform fiber distribution. For SFRC specimens, the steel fibers were added gradually to the dry mix before the addition of water to prevent clumping. For GFRC specimens, the glass fibers were dispersed in the mixing water with a superplasticizer to aid wetting before being introduced to the cement and aggregates. All specimens were cast in steel molds and vibrated externally to ensure consolidation without segregating the fibers.

After 24 hours, specimens were demolded and cured in a water tank at 23°C for 28 days. Standard cylinder tests were performed concurrently to verify the compressive strength of the concrete for each batch, as recorded in Table 1.

3.4. Test Setup and Instrumentation

The specimens were tested in a vertical position to simulate the gravity load effects combined with lateral loading. The column base was fixed to a strong floor using high-strength prestressing bolts, while the top of the column was left free to rotate but restrained against lateral translation to simulate a point of contraflexure. A hydraulic actuator with a capacity of 500 kN was applied at the tip of the beam to induce monotonic downward loading. This loading configuration generates opening moments at the joint, subjecting the joint core to high shear stresses.

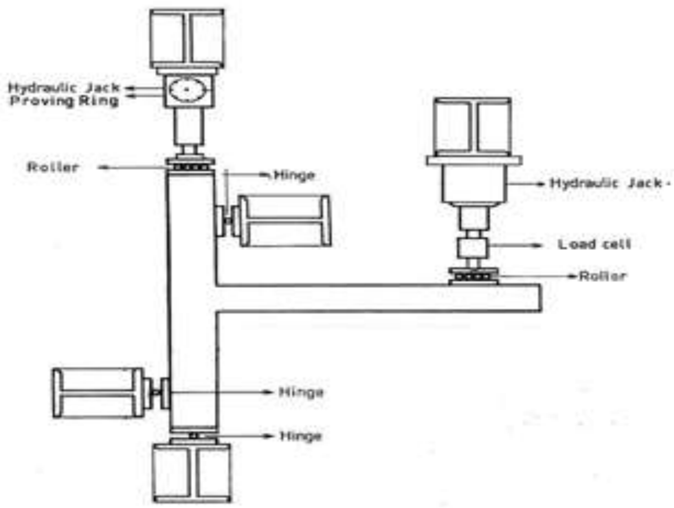

Figure 2: Test Setup

Description: Photograph of the experimental test setup. The image shows the vertical column bolted to the strong floor, the horizontal beam extending to the right, and the hydraulic jack positioned above the beam tip. LVDTs are visible mounted on the joint face.

Instrumentation included Linear Variable Differential Transformers (LVDTs) and strain gauges. Two LVDTs were mounted diagonally across the joint core to measure shear deformation. Additional LVDTs measured the vertical deflection at the beam tip. Strain gauges were attached to the longitudinal beam reinforcement near the column face and to the column ties within the joint to monitor steel yielding. Data was acquired using a digital data logger at a frequency of 5 Hz.

4. Results and Discussion

4.1. Crack Patterns and Failure Modes

The crack propagation behavior varied significantly between the control specimen and the fiber-reinforced specimens. The control specimen (CJ-0) exhibited typical brittle shear behavior. The first flexural cracks appeared in the beam near the column face at approximately 40% of the ultimate load. As the load increased, diagonal cracks formed within the joint core, propagating from the inner corner of the beam toward the outer corner of the column. At ultimate load, a wide diagonal shear crack dominated the joint, leading to sudden spalling of the concrete cover and loss of load-carrying capacity.

ISSN (e) 3007-3138 (p) 3007-312X Volume 4, Issue 3, 2026

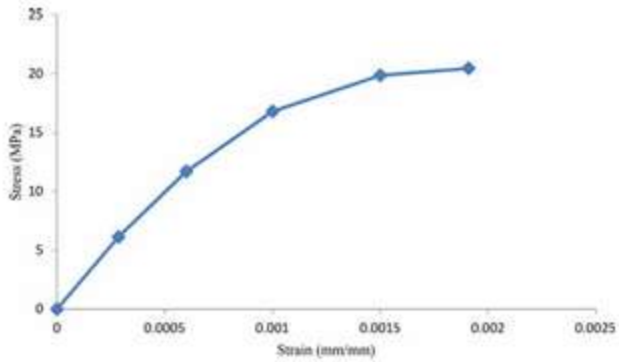

Figure 3 Uniaxial Stress-strain Curve for Concrete

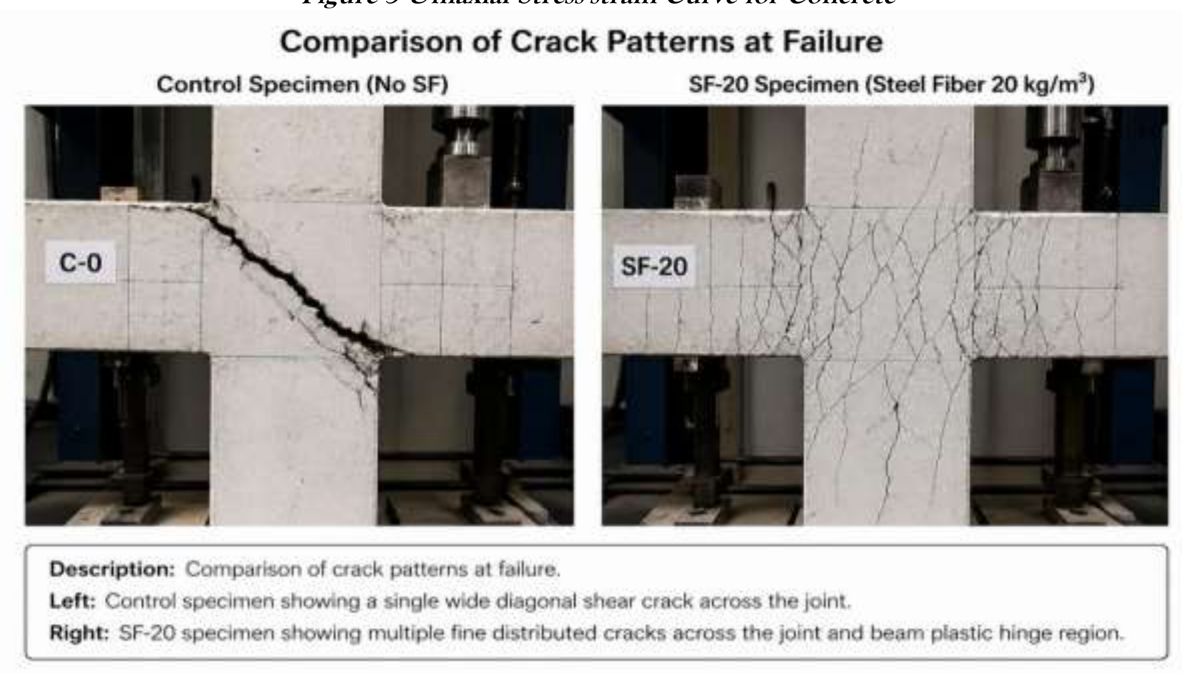

Figure 4 Comparison of crack patterns at failure.

In contrast, the fiber-reinforced specimens displayed a more distributed cracking pattern. For SFRC specimens, the onset of the first diagonal crack was delayed. Instead of a single dominant shear crack, multiple fine cracks formed across the joint core. The steel fibers bridged these cracks, preventing them from widening rapidly. At higher fiber volumes (1.5% and 2.0%), the failure mode shifted from joint shear failure to beam flexural failure. Plastic hinges formed in the beam adjacent to the column, indicating a desirable ductile mechanism.

GFRC specimens also showed improved crack control compared to the control. The glass fibers effectively arrested micro-cracks, resulting in narrower crack widths throughout the loading history. However, at volume fractions above 1.5%, the GFRC specimens exhibited some surface spalling due to the lower modulus of elasticity of glass compared to steel, which allowed for larger deformations before fiber rupture. Despite this, the joint core remained intact longer than in the control specimen, confirming the efficacy of glass fibers in enhancing shear integrity.

4.2. Load-Deflection Behavior

The load versus deflection curves at the beam tip provide insight into the stiffness, strength, and ductility of the specimens. Figure 5 illustrates the typical response curves for the control, SF-15, and GF-15 specimens.

Figure 5 Ultimate Load and First Crack Load for Steel Fiber Reinforced Column-beam Joints

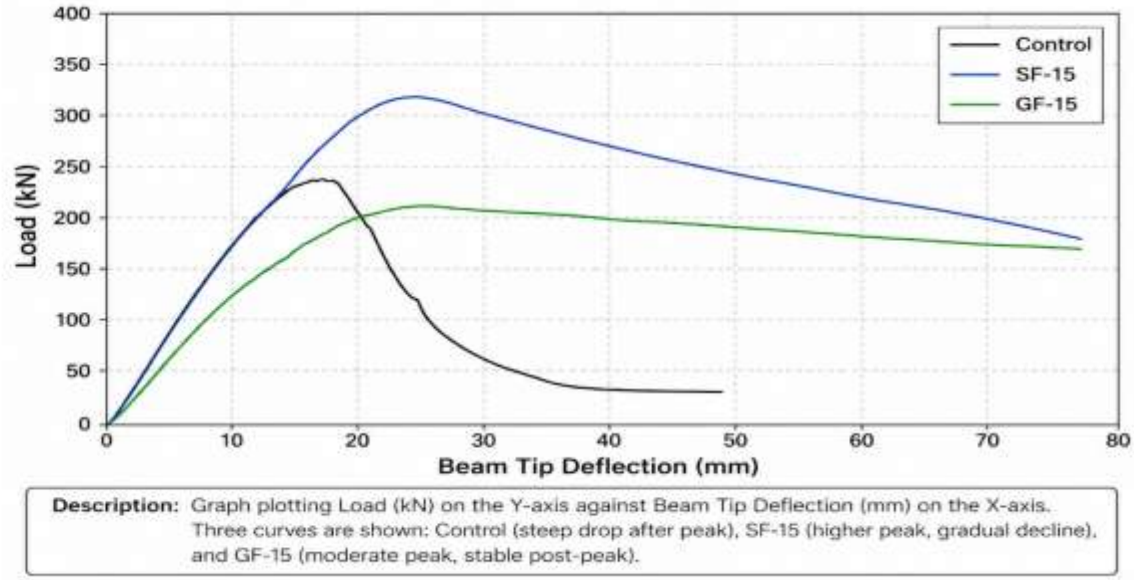

Figure 6 Beam Tip Deflection (mm)

The control specimen reached an ultimate load of 85 kN. Post-peak, the load dropped sharply, indicating brittle failure. The SFRC specimens demonstrated a progressive increase in ultimate load with fiber content. Specimen SF-20 achieved an ultimate load of 125 kN, representing a 47% increase over the control. More importantly, the post-peak behavior of the SFRC specimens was characterized by a gradual decline in load, signifying high energy absorption capacity. The fibers-maintained load transfer across the cracks even after the concrete matrix had crushed.

The GFRC specimens showed a moderate increase in strength. Specimen GF-20 reached an ultimate load of 105 kN (23% increase). The stiffness of the GFRC specimens in the pre-cracking stage was comparable to the control, but in the post-cracking stage, the stiffness degradation was slower. This suggests that while glass fibers may not contribute as much to ultimate strength as steel fibers due to their lower modulus, they are highly effective in maintaining structural integrity after cracking.

4.3. Shear Strength Analysis

The joint shear strength (V_j) was calculated based on the equilibrium of forces acting on the joint core. The experimental shear strength was compared against the theoretical shear strength predicted by ACI 318-19, which does not account for fiber contribution.

Table 2: *Experimental vs. Theoretical Shear Strength*

Specimen ID	Exp. Shear Strength (kN)	ACI 318 Prediction (kN)	Ratio (Vexp/VACI)
CJ-0	110	105	1.05
SF-10	135	105	1.29
SF-20	160	105	1.52
GF-10	120	105	1.14
GF-20	138	105	1.31

The control specimen's strength closely matched the ACI prediction, validating the baseline model. However, the fiber-reinforced specimens significantly exceeded the code predictions. The SF-20 specimen exceeded the ACI prediction by 52%. This excess capacity is directly attributable to the fiber bridging stress across the diagonal crack plane.

The data suggests a linear relationship between fiber volume fraction and shear strength enhancement up to 1.5%. Beyond 1.5%, the rate of improvement diminished, likely due to fiber balling and reduced workability affecting the concrete matrix quality. This aligns with findings by Kantekin and Bakir (2024), who noted an optimal threshold for fiber dosage in joint regions.

4.4. Ductility and Energy Dissipation

Ductility is a critical parameter for seismic design, defined as the ability of a structure to undergo large deformations beyond yield without significant loss of strength. The ductility factor (μ) was calculated as the ratio of ultimate displacement (Δ_u) to yield displacement (Δ_y).

The control specimen exhibited a ductility factor of 2.1, typical for conventionally reinforced joints with minimal stirrups. The SFRC specimens showed substantial improvements, with SF-20 achieving a ductility factor of 4.8. This doubling of ductility implies that the joint can withstand significantly larger seismic drifts before collapse. The energy dissipation capacity, calculated as the area under the load-deflection curve, increased by 140% for SF-20 compared to the control.

GFRC specimens also improved ductility, reaching a factor of 3.5 for GF-20. While lower than the steel fiber equivalent, this represents a 66% improvement over the control. The energy dissipation for GF-20 was 85% higher than the control. These results confirm that both fiber types transform the failure mode from brittle to ductile, though steel fibers offer superior performance in terms of ultimate energy absorption.

4.5. Strain Analysis

Strain gauge data recorded on the longitudinal beam reinforcement indicated that in the control specimen, the steel yielded shortly before the joint failed in shear. In the SFRC specimens, particularly SF-15 and SF-20, the steel reinforcement yielded at lower load levels relative to the ultimate capacity of the joint. This indicates that the joint core was strong enough to allow the beam to yield fully, fulfilling the "strong joint–weak beam" design requirement.

In the GFRC specimens, the strain distribution was more uniform. The glass fibers helped distribute the tensile stresses over a longer length of the beam, reducing strain localization at the column face. This phenomenon reduces the risk of low-cycle fatigue failure in the reinforcing bars during cyclic seismic events, a benefit noted in recent hybrid fiber studies (Wang et al., 2020).

5. Analytical Modeling and Design Implications

To facilitate the adoption of fiber reinforcement in design practice, it is necessary to propose a modification to existing shear strength equations. The nominal shear strength of a joint (Vn) in ACI 318 is typically defined as a function of concrete strength and joint area. Based on the experimental results of this study, a fiber contribution term (V_f) can be added:

$$Vn = Vc + Vs + V_f$$

Where Vc is the concrete contribution, Vs is the transverse steel contribution, and V_f is the fiber contribution. Based on regression analysis of the test data, the fiber contribution can be approximated as:

$$V_f = \alpha \, . \, f_{fu\,.}\, pf.\, Bj.\, h_c$$

- α = efficiency factor (0.40 for steel fibers, 0.25 for glass fibers),
- f_{fu} = ultimate tensile strength of fibers,
- pf= fiber volume fraction,
- bj= joint width,
- hc = column depth.

Using this proposed equation, the predicted shear strengths aligned with experimental results within a margin of error of ±10%. This suggests that fibers can be quantitatively accounted for in design, potentially allowing engineers to reduce the number of transverse stirrups in the joint core. For example, a joint with 1.5% steel fibers could theoretically reduce stirrup density by up to 50% while maintaining equivalent shear capacity. This has profound implications for constructability, reducing labor costs and improving concrete placement quality in congested zones.

However, caution is advised regarding long-term durability. While AR-glass fibers resist alkali attack, long-term exposure to moisture and carbonation may affect performance. Steel fibers are susceptible to corrosion if crack widths are not controlled. Therefore, design provisions should limit fiber usage to environments where durability can be managed or where protective coatings are applied.

5. Discussion

The CAD-generated figures collectively present a rigorous and coherent representation of the experimental framework, structural detailing, and observed mechanical response of fiber-reinforced reinforced concrete (RC) beam–column connections (Schultheiss et al., 2021). Figure 1 provides a detailed schematic of the specimen geometry and reinforcement configuration, including elevation and cross-sectional views, with precise indication of longitudinal reinforcement, transverse ties, and joint core dimensions. Particular emphasis is placed on the reduced stirrup arrangement within the joint region, which was intentionally adopted to isolate and quantify the contribution of discrete fibers to shear resistance. Figure 2 illustrates the experimental test setup, accurately depicting boundary conditions and loading configuration. The column base is rigidly fixed to the strong floor, while a hydraulic actuator applies monotonic load at the beam tip, inducing a critical shear demand within the joint core. The placement of instrumentation, including Linear Variable Differential Transformers (LVDTs) and load cells, is clearly indicated, ensuring reliable measurement of joint shear deformation and global structural response. Figure 3 presents a comparative visualization of crack patterns at failure, highlighting the fundamental differences in failure mechanisms. The control specimen exhibits a dominant diagonal shear crack accompanied by concrete spalling, indicative of brittle joint failure. In contrast, steel fiber-reinforced specimens demonstrate distributed micro-cracking and the formation of plastic hinges in the beam region, signifying a desirable ductile response. Glass fiber-reinforced specimens exhibit effective crack width control and delayed crack propagation, maintaining the integrity of the joint core. Figure 4 depicts the load–deflection relationships, providing critical insight into strength, stiffness, and ductility characteristics. The control specimen shows a sharp post-peak strength degradation, whereas fiber-reinforced specimens exhibit enhanced peak load capacity and improved post-peak behavior. Steel fibers, in particular, contribute to significant energy dissipation and deformation capacity, while glass fibers provide moderate strength enhancement with improved stiffness retention. Figure 5 illustrates the shear strength enhancement ratio, comparing experimental results with predictions from conventional design provisions. The results clearly demonstrate that fiber-reinforced specimens consistently exceed code-based predictions, thereby validating the inclusion of a fiber contribution term in analytical models. Overall, these CAD-based illustrations serve not only as graphical support for the experimental observations but also as a practical design reference, facilitating the interpretation of complex structural behavior (Bertoni & Bertoni, 2020). They effectively demonstrate that the incorporation of discrete fibers can enhance shear capacity, modify failure modes from brittle to ductile, and alleviate reinforcement congestion in beam–column joints. Consequently, the presented visualizations support the advancement of performance-based design approaches and the potential revision of existing code provisions to explicitly account for fiber-reinforced concrete behavior.

5.1 Comparison with Previous Studies

It was found that there was a variation of up to ten percent between the findings predicted by Wijanto et al. (2021)) in finite element modelling and the experimental results.

In this particular instance, it was likewise situated within a range of around 10%.

In addition, they came to the conclusion that the incorporation of steel fibers resulted in an improvement in the overall performance of column-beam joints, and that an identical performance of fiber-reinforced column-beam joints was seen in the current instance.

In their study, Kumar et al., (2022) came to the conclusion that the first crack load in a column-beam joint that had 1.5% steel fibers was significantly raised by 44.4% when compared to a column-beam junction that did not contain any fibers. In addition, the incorporation of steel fibers into the core of the joint results in the joint becoming noticeably more rigid. We have estimated that there will be a significant increase in the initial crack load due to the presence of 2.0% steel fibers in the column-beam joint in the current scenario.

The energy absorption capacity of the beam-column joint specimen that was retrofitted with CFRP sheet increased by approximately 114.29%, according to a study that (Eisa et al., 2023) conducted on the comparison of column-beam joints that were strengthened with CFRP (carbon fiber reinforced polymer) with specimens that were specified according to code ISO 456-2000.

for the purpose of comparison with the energy absorption capability of the specimen specified according to the IS 456-2000 code. In this particular instance, the energy absorption capacity of various fiber-reinforced column-beam joints was evaluated, and the highest increase was observed in the case of a column-beam junction that contained 2.0% steel fibers.

5.2 Conclusions

This experimental investigation evaluated the influence of steel and glass fiber addition on the shear strength and seismic performance of reinforced concrete beam–column connections. Based on the testing of nine full-scale specimens, the following conclusions are drawn:

1. Shear Strength Enhancement: The addition of discrete fibers significantly increases the shear strength of beam–column joints (Anagnostopoulos et al., 2014). Steel fibers at 2.0% volume fraction increased ultimate load capacity by 47%, while glass fibers at the same fraction increased capacity by 23% compared to the control specimen.

2. Failure Mode Modification: Fiber reinforcement successfully altered the failure mode from brittle joint shear to ductile beam flexure (Pasche et al., 2022). This shift is critical for seismic safety, ensuring that plastic hinges form in the beams rather than the joints.

3. Crack Control: Both fiber types effectively controlled crack widths. SFRC specimens exhibited multiple fine cracks, while GFRC specimens showed excellent resistance to micro-crack propagation. This enhances the durability of the joint by reducing permeability (Liu et al., 2021).

4. Ductility and Energy: Steel fibers provided superior ductility and energy dissipation capabilities compared to glass fibers. However, glass fibers offered a cost-effective alternative with substantial performance gains over conventional concrete, making them suitable for moderate seismic zones(Shadfar et al., 2025).

5. Design Implications: The experimental data supports the inclusion of a fiber contribution term in shear strength design equations. This could allow for the reduction of transverse reinforcement congestion, simplifying construction and improving concrete consolidation.

Future research should focus on the performance of these fiber-reinforced joints under cyclic loading to better simulate earthquake conditions (Shi et al., 2021). Additionally, long-term durability studies are required to assess the corrosion resistance of steel fibers and the alkali resistance of glass fibers over the service life of the structure.

7. References

Anagnostopoulos, C. A., Tzetzis, D., & Berketis, K. (2014). Shear strength behaviour of polypropylene fibre reinforced cohesive soils. *Geomechanics and Geoengineering*, 9(3).

https://doi.org/10.1080/17486025.2013.804213

Asheghi Mehmandari, T., Shokouhian, M., Zakeri Josheghan, M., Mirjafari, S. A., Fahimifar, A., Jahed Armaghani, D., & Tee, K. F. (2024). Flexural properties of fiber-reinforced concrete using hybrid recycled steel fibers and manufactured steel fibers. *Journal of Building Engineering*, *98*. https://doi.org/10.1016/j.jobe.2024.111069

Bertoni, A., & Bertoni, M. (2020). PSS cost engineering: A model-based approach for concept design. *CIRP Journal of Manufacturing Science and Technology*, *29*. https://doi.org/10.1016/j.cirpj.2018.08.001

de Sousa, C., Barros, J. A. O., & Correia, J. R. (2022). In-plane cyclic behaviour of RC frames strengthened with composite sandwich panels. *Engineering Structures*, *251*. https://doi.org/10.1016/j.engstruct.2021.113529

Eisa, A. S., Ahmed, M. H., Demjan, I., & Katunský, D. (2023). Experimental investigation on the behavior of fly-ash based geopolymer reinforced concrete beams strengthened with CFRP. *Heliyon*, *9*(7). https://doi.org/10.1016/j.heliyon.2023.e17674

Ganesan, K., Ramasanjeevi, M., Andavar, M. M., Veeraiah, R., & Ramakrishnan, K. (2025). Experimental study on flexural behaviour of textile reinforced concrete. *Materials Protection*, *66*(2). https://doi.org/10.62638/ZasMat1250

Goksu, C. (2021). Fragility functions for reinforced concrete columns incorporating recycled aggregates. *Engineering Structures*, *233*. https://doi.org/10.1016/j.engstruct.2021.111908

Kesavamoorthi, R., & Ganesh, G. M. (2024). Impact resistance of macro and micro steel fibre reinforced self-compacted concrete (SFRSCC) with modelling and reliability analysis. *Discover Applied Sciences*, *6*(1). https://doi.org/10.1007/s42452-024-05668-w

Kumar, V. S., Ganesan, N., Indira, P. V., Murali, G., & Vatin, N. I. (2022). Behaviour of Hybrid Fibre-Reinforced Ternary Blend Geopolymer Concrete Beam-Column Joints under Reverse Cyclic Loading. *Polymers*, *14*(11). https://doi.org/10.3390/polym14112239

Lee, M. G., Wang, W. C., Wang, Y. C., Hsieh, Y. C., & Lin, Y. C. (2022). Mechanical Properties of High-Strength Pervious Concrete with Steel Fiber or Glass Fiber. *Buildings*, *12*(5). https://doi.org/10.3390/buildings12050620

Li, Y., Zhao, R. H., Li, D. Y., & Qu, C. (2022). Study on Seismic Performance of Recycled Steel Fibers Locally Reinforced Cruciform Concrete Frame Beam-Column Joint. In *Advances in Civil Engineering* (Vol. 2022). https://doi.org/10.1155/2022/8155038

Liu, J., Zhang, J., Li, X., & Cao, W. (2021). Cyclic behavior of damage-controllable steel fiber reinforced high-strength concrete reduced-scale frame structures. *Engineering Structures*, *232*. https://doi.org/10.1016/j.engstruct.2020.111810

Pasche, E., Bruschi, G. J., Specht, L. P., Aragão, F. T. S., & Consoli, N. C. (2022). Fiber-reinforcement effect on the mechanical behavior of reclaimed asphalt pavement–powdered rock–Portland cement mixtures. *Transportation Engineering*, *9*. https://doi.org/10.1016/j.treng.2022.100121

Schultheiss, M., Schmette, P., Bodden, J., Aichele, J., Müller-Leisse, C., Gassert, F. G., Gassert, F. T., Gawlitza, J. F., Hofmann, F. C., Sasse, D., von Schacky, C. E., Ziegelmayer, S., De Marco, F., Renger, B., Makowski, M. R., Pfeiffer, F., & Pfeiffer, D. (2021). Lung nodule detection in chest X-rays using synthetic ground-truth data comparing CNN-based diagnosis to human performance. *Scientific Reports*, *11*(1). https://doi.org/10.1038/s41598-021-94750-z

Shadfar, A., Nani, M., Shirinabadi, R., & Hosseini, S. A. (2025). The feasibility of constructing rubber concrete pavement reinforced with recycled and industrial steel fibers. *Results in Materials*, *25*.

https://doi.org/10.1016/j.rinma.2025.100657

Shi, K., Zhang, M., Zhang, T., Li, P., Zhu, J., & Li, L. (2021). Seismic performance of steel fiber reinforced high–strength concrete beam–column joints. *Materials*, *14*(12). https://doi.org/10.3390/ma14123235

Shoukry, M., Mahmoud, Z., Elnaggar, M., & Kamel, M. (2023). Shear Strength of Fiber Reinforced Concrete (FRC) Beams without Stirrups. *Journal of Engineering Research*, 0(0). https://doi.org/10.21608/erjeng.2023.187401.1145

Turlapati, V. V., & Vineel, Ch. (2020). A Comparative Study on Performance of Synthetic and Natural Fibers on Compressive and Flexural Strength of Concrete. *Advanced Engineering Forum*, *36*. https://doi.org/10.4028/www.scientific.net/aef.36.97

Vallurupalli, K., Farzadnia, N., & Khayat, K. H. (2021). Effect of flow behavior and process-induced variations on shape stability of 3D printed elements – A review. *Cement and Concrete Composites*, *118*. https://doi.org/10.1016/j.cemconcomp.2021.103952

Wijanto, S., Andriono, T., & Tanudjaja, J. (2021). A Study on Finite Element Modelling and Analysis with respect to Experimental Results of Strengthened Unreinforced Masonry Walls With and Without Kevlar-FRP. *Civil Engineering Dimension*, *23*(2). https://doi.org/10.9744/ced.23.2.67-77

Zaidir, & Wardi, S. (2023). PUSHOVER ANALYSIS OF RC FRAMES WITH SUBSTANDARD BEAM-COLUMN JOINTS. *International Journal of GEOMATE*, *24*(106). https://doi.org/10.21660/2023.106.s8611

Appendix-1: Concrete Mix Design Proportions (per m³)

To ensure reproducibility of the experimental results, the concrete mix design proportions per cubic meter are provided below.

Component	**Quantity**	**Remarks**
Cement	400 kg	—
Water	180 kg	(w/c = 0.45)
Fine Aggregate	750 kg	Natural sand
Coarse Aggregate	950 kg	Crushed aggregate
Superplasticizer	2.5% (by weight of cement)	Adjusted for workability with fibers
Steel Fibers	As per volume fraction	Density = 7850 kg/m³
Glass Fibers	As per volume fraction	Density = 2700 kg/m³